Since January 2020 Elsevier has created a COVID-19 resource centre with free information in English and Mandarin on the novel coronavirus COVID-19. The COVID-19 resource centre is hosted on Elsevier Connect, the company's public news and information website.

Energy 230 (2021) 120876

Contents lists available at ScienceDirect

Energy

journal homepage: www.elsevier.com/locate/energy

COVID-19 mask waste to energy via thermochemical pathway: Effect of Co-Feeding food waste

Chanyeong Park [a], Heeyoung Choi [b], Kun-Yi Andrew Lin [c], Eilhann E. Kwon [d, *], Jechan Lee [a, b, **]

[a] Department of Energy Systems Research, Ajou University, 206 World Cup-ro, Suwon, 16499, Republic of Korea
[b] Department of Environmental and Safety Engineering, Ajou University, 206 World Cup-ro, Suwon, 16499, Republic of Korea
[c] Department of Environmental Engineering & Innovation and Development Center of Sustainable Agriculture, National Chung Hsing University, 250 Kuo-Kuang Road, Taichung, 402, Taiwan
[d] Department of Environment and Energy, Sejong University, 209 Neungdong-ro, Seoul, 05006, Republic of Korea

ARTICLE INFO

Article history:
Received 4 March 2021
Received in revised form
19 April 2021
Accepted 4 May 2021
Available online 7 May 2021

Keywords:
Thermochemical pathway
Pyrolysis
Co-feeding
Disposable waste
Municipal solid waste (MSW)
Waste valorization

ABSTRACT

In this study, co-pyrolysis of single-use face mask (for the protection against COVID-19) and food waste was investigated for the purpose of energy and resource valorization of the waste materials. To this end, disposable face mask (a piece of personal protective equipment) was pyrolyzed to produce fuel-range chemicals. The pyrolytic gas evolved from the pyrolysis of the single-use face mask consisted primarily of non-condensable permanent hydrocarbons such as CH_4, C_2H_4, C_2H_6, C_3H_6, and C_3H_8. An increase in pyrolysis temperature enhanced the non-condensable hydrocarbon yields. The pyrolytic gas had a HHV of >40 MJ kg^{-1}. In addition, hydrocarbons with wider carbon number ranges (e.g., gasoline-, jet fuel-, diesel-, and motor oil-range hydrocarbons) were produced in the pyrolysis of the disposable face mask. The yields of the gasoline-, jet fuel-, and diesel-range hydrocarbons obtained from the single-use mask were highest at 973 K. The pyrolysis of the single-use face mask yielded 14.7 wt% gasoline-, 18.4 wt% jet fuel-, 34.1 wt% diesel-, and 18.1 wt% motor oil-range hydrocarbons. No solid char was produced via the pyrolysis of the disposable face mask. The addition of food waste to the pyrolysis feedstock led to the formation of char, but the presence of the single-use face mask did not affect the properties and energy content of the char. More H_2 and less hydrocarbons were produced by co-feeding food waste in the pyrolysis of the disposable face mask. The results of this study can contribute to thermochemical management and utilization of everyday waste as a source of energy.

1. Introduction

The COVID-19 pandemic has resulted in exacerbating plastic pollution. Heavy dependence upon take-away and hygiene concerns leading to employing personal protective equipment has increased the use of plastics; however, measures proposed to reduce plastic use, such as (e.g., banning single-use plastic bags) have been paused, rolled back, and even banned. Single-use face masks are the most common personal protective equipment to prevent the spread of the pandemic. The employment of single-use face masks has become widespread because many national and local governments have mandated the public wear masks. In 2019, the global market size of face masks was about 0.8 billion USD, but it was expanded to about 166 billion USD at the end of 2020 [1,2]. The skyrocketing demand for face masks enormously increases face mask waste. However, they are difficult to be recycled owing to their complex compositions and the risk of COVID-19 infection. In many cases, used masks are improperly discarded mostly because increased volume of the waste overwhelms waste management systems [3]. A substantial portion of the improperly discarded face masks enter the ocean and pollute marine ecosystems. According to an estimation by OceansAsia, in 2020 approximately 1.6 billion masks enter the ocean, equivalent to 4700–6200 tons of plastic pollution [4].

Food waste is another global challenge. People waste about a third of all food produced for human consumption [5]. Food waste

* Corresponding author.
** Corresponding author. Department of Energy Systems Research, Ajou University, 206 World cup-ro, Suwon, 16499, Republic of Korea
E-mail addresses: ekwon74@sejong.ac.kr (E.E. Kwon), jlee83@ajou.ac.kr (J. Lee).

https://doi.org/10.1016/j.energy.2021.120876
0360-5442/

has not only taken loads of fresh water, land, and labor to produce, but also been bad for the environment including climate. Most food waste in developing regions is down to infrastructure, but it is down to consumer levels in developed countries. The decrease in food waste can reduce global greenhouse gas emissions [6]. According to a working paper prepared by Climate Focus and International Institute for Applied Systems Analysis, a reduction in food waste provides significant greenhouse gas mitigation at approximately 0.38–4.5 Gt of CO_2 equivalent per year [7].

In this regard, both disposable face masks and food waste must be carefully treated. Given that both are kinds of everyday waste, it is preferable to simultaneously treat the mask and food waste. Co-pyrolysis (a process to pyrolyze two or more different materials as a feedstock) is a promising optional technique to valorize a range of carbonaceous substances [8]. For instance, co-pyrolysis of biomass and plastic is a major pathway for upgrading bio-oil, which enhances the yield and quality of bio-oil because of high C and H contents and low O content of plastics [9]. Compared to other bio-oil upgrading methods (e.g., hydrogenation, hydrodeoxygenation [10,11], and catalytic pyrolysis [12,13]), co-pyrolysis is simple and safe because it does not require high-pressure hydrogen (it operates under ambient pressure without supplying hydrogen) [14]. In addition, the ratio of cost to performance for co-pyrolysis process is low [15]. For the reasons, co-pyrolysis of biomass and plastic is considered an effective upgrading method of pyrolytic products. Recently, there has been efforts to apply co-pyrolysis to simultaneously treating different waste materials (organic waste, waste plastics, etc.) [16].

There have been few papers relevant to pyrolysis of disposable face masks and polymers that are used on disposable face masks. In Table S1, the yields of pyrolytic products produced via pyrolysis of disposable face mask [17,18], hospital plastic waste [19,20], and polymers that might be used to make disposable face masks [21,22] are compared. However, co-pyrolysis of single-use face mask and organic waste has not been reported yet. Here in this study, we have first reported co-pyrolysis of single-use face mask and food waste. Considering that disposable face masks are made of a range of melt-blown plastic materials, co-pyrolysis of the mask and food waste would be beneficial to their valorization to energy and value-added chemicals. The aim of this study was to investigate the effect of using food waste as co-feedstock of disposable face mask pyrolysis on the characteristics of gas, liquid, and solid pyrolytic products. The characteristics of the pyrolytic products are described based both on their heating values and on the carbon number ranges of different fuels and oils. This research should contribute to innovating approaches to valorize wastes produced by different sectors to transform our society towards a sustainable and zero-waste environment.

2. Materials and methods

2.1. Feedstock

Single-use face masks (Korea filter 94 grade) were purchased from a local pharmacy near Ajou University campus. The mask sample was dried at 333 K overnight to remove moisture prior to its use as the feedstock. Food waste was supplied by a waste treatment facility in Suwon, Gyeonggi, Republic of Korea. It was dewatered using a screw press, followed by magnetic separation of any impurities. After that, the food waste sample was dried at 333 K overnight. All chemical reagents were purchased from Sigma-Aldrich (St. Louis, MO, USA).

2.2. Pyrolysis experimental setup

A pyrolysis experimental setup used in this study is depicted in Figure S1. It comprised a split-hinge tube furnace, a temperature controller, a quartz tube (length: 0.6 m, outside diameter: 25 mm, and wall thickness: 4 mm), a mass flow controller, and a condensable trap composed of an ice bath (272 K) and a dry ice/acetone bath (223 K). During the pyrolysis and co-pyrolysis, an oxygen-free environment was controlled by the mass flow controller to flow ultra-high purity N_2 gas (100 mL min^{-1}). For pyrolysis experiments, about 2.25 g of mask (filters: 1.79 g; ear rope: 0.22 g; nose wire: 0.24 g) was used as the feedstock. Sieved size of food waste was between 0.6 mm and 1.0 mm. Feedstock loading in the reactor is pictured in Figure S1. Each experiment was carried out in triplicate to check the reproducibility of experimental results.

2.3. Pyrolytic product analysis

Permanent gases (i.e., non-condensable gases) evolved from the pyrolysis and co-pyrolysis were quantified by using a micro gas chromatograph (GC) (model: Fusion Gas Analyzer) manufactured by INFICON (Bad Ragaz, Switzerland). The micro GC was directly connected to the reactor outlet (Figure S1), which allowed in-situ analysis of the gaseous products. Specification and product analysis conditions of the micro GC are provided in Table S2.

Chemical compounds in condensable products were identified and quantified by using a GC–mass spectrometry (GC–MS) (GC model: 7890 A; MS model: 5975C) manufactured by Agilent Technologies (Santa Clara, CA, USA). For the identification of condensable species, each peak shown in GC–MS chromatograms was matched with the NIST mass spectral library, which area was integrated separately. A 10 ng mL^{-1} of 5-methylfurfural was used as an internal standard to calculate concentrations of the identified species. Table S3 gives specification and product analysis conditions of the GC–MS.

The residual solids after the pyrolysis and co-pyrolysis were also characterized. Their specific surface area and porosity were determined through N_2 physisorption conducted at 77 K using a volumetric adsorption analyzer (model: BELSORP mini II) manufactured by MicrotracBEL (Osaka, Japan). Degassing the sample was performed before the physisorption as follows: at 363 K for 30 min and then at 423 K under vacuum. BET (Brunauer, Emmett, and Teller) theory was applied to determining specific surface area, and BJH (Barrett, Joyner, and Halenda) desorption method ($P/P_0 = 0.99$) was employed to determine pore volume and size. Elemental composition of the solid residue was analyzed by its combustion at 1273 K in the presence of copper wire and tungsten(VI) oxide catalysts in a elemental analyzer (model: FlashSmart 2000) manufactured by Thermo Scientific (Waltham, MA, USA). Ash content of the solid residue was analyzed by heating the sample at 1023 K for 1 h in an open-top crucible. Higher heating value (HHV) of the char was calculated based on its elemental composition using Eq. (1):

$$HHV = 34.91X_C + 117.83X_H + 10.05X_S - 10.34X_O - 1.51X_N - 2.11X_{Ash} \quad \text{(Eq. 1)}$$

where X_C, X_H, X_S, X_O, X_N, and X_{Ash} are the fraction of carbon, hydrogen, sulfur, oxygen, nitrogen, and ash of char (by weight) [23].

3. Results and discussion

3.1. Feedstock characterization

The single-use face mask was composed of filter parts made of polypropylene (PP), ear straps made of polyamide and polyurethane, and a nose bridge strip made of aluminum metal. The nose bridge strip was removed before the pyrolysis of the disposable COVID-19 mask. Table 1 summarizes the results of proximate

and ultimate analyses for the mask. It contained mostly volatile species. Oxygen and nitrogen likely originated from polyamide and polyurethane of which the ear straps are made. As present in Table 1, the food waste had a high level of oxygen content, 41.6 wt%. It contained sulfur of 0.4 wt%, while the mask did not contain sulfur. Nitrogen contained in the food waste should originate from amino acids [24,25]. The food waste was composed of cellulose, hemicellulose, and lignin of 3.3 wt% and extractives (lipids, fatty acids, fatty alcohols, amino acids, phosphates, etc. [26,27]) of 96.7 wt%.

3.2. Pyrolysis of disposable COVID-19 mask

The overall mass balances of the pyrolytic products made from the single-use face mask are shown in Fig. 1. The total yield of the pyrolytic gas composed of non-condensable permanent gases (e.g., methane (CH_4), ethane (C_2H_6), propane (C_3H_8), ethylene (C_2H_4), propylene (C_3H_6), carbon monoxide (CO), carbon dioxide (CO_2), and hydrogen (H_2)) was enhanced from 2.4 wt% to 5.4 wt% with an increase in the pyrolysis temperature from 773 K to 1173 K. At high temperatures, thermal cracking of the condensable pyrolytic vapor was promoted by gas phase homogeneous reactions and heterogeneous reactions taking place between pyrolytic vapor and the feedstock during the pyrolysis [28,29]. On a per mass basis, 52–59% of the disposable face mask was converted into condensable species (collected by the condensable trap; Figure S1) at all temperatures tested. The species that were not collected by the trap but not the permanent gases are considered volatiles (which may be too highly volatile to be condensed in the trap). No solid residue (i.e., char) was observed after the pyrolysis. This shows a complete thermal degradation of the mask at temperatures higher than 773 K.

The product distributions in the non-condensable permanent gases produced from the disposable COVID-19 mask at different pyrolysis temperatures are represented in Fig. 2. The gases were hydrogen (H_2), methane (CH_4), ethylene (C_2H_4), ethane (C_2H_6), propylene (C_3H_6), propane (C_3H_8), carbon monoxide (CO), and CO_2. On the weight basis per the feedstock, C_3H_6 was the most produced non-condensable gas for the pyrolysis of the COVID-19 mask, which obviously resulted from depolymerization of PP that comprises the mask filter layers. Disproportionation of C_3H_6 resulted in the formation of C_2H_4 [30]. Note that the conversion of C_3H_6 into C_2H_4 reported in earlier literature has undertaken with catalysts such as metal oxides [30] and zeolites [31]. However, such disproportionation reaction can thermally occur [32], which should give lower selectivity than catalytic reaction. H_2 was generated likely via dehydrogenation reactions occurring in the pyrolysis [33]. Hydrogenation of C_2H_4 and C_3H_6 with the hydrogen generated during the pyrolysis resulted in C_2H_6 and C_3H_8, respectively. CH_4, CO, and CO_2 could be produced via thermal cracking of pyrolytic vapor [34].

The HHVs of the gaseous pyrolytic products obtained at different temperatures were calculated based on the heat of the combustion of each gas and the amount of the gaseous products produced. The HHV increased from 40.7 MJ kg^{-1} to 43 MJ kg^{-1} as the pyrolysis temperature increased from 773 K to 973 K. A further increase in the temperature from 973 K to 1173 K did not significantly raise the HHV.

The hydrocarbons identified in the pyrolytic liquid produced from the single-use face mask via pyrolysis ranged from C6 to C28 (Table 2). They could be classified as gasoline-range hydrocarbons (C4–C12), jet fuel-range hydrocarbons (C5–C14), diesel-range hydrocarbons (C8–C21), and motor oil-range hydrocarbons (C18–C35). Table S4 illustrates the carbon chain lengths of hydrocarbons associated with different fuel and oil formulations and how these affect their boiling points. An increase in the number of carbons makes intermolecular attractive forces cumulatively more considerable, resulting in high boiling points. As shown in Fig. 3, the yields of gasoline-, jet fuel-, diesel-, and motor oil-range hydrocarbons were highest at 973 K. At temperatures lower than 973 K, thermal cracking of chemical compounds that have higher molecular weights than the C6–C28 hydrocarbons might not be enough, thereby bigger molecules than the C6–C28 species existing in the pyrolytic liquid. However, more thermal cracking occurs at temperatures higher than 973 K, lowering the yields of gasoline-, jet fuel-, diesel-, and motor oil-range hydrocarbons. Table S5 gives HHVs of the gasoline-, jet fuel-, diesel-, and motor oil-range hydrocarbons calculated with an assumption of heat of combustion of *n*-alkanes having corresponding carbon numbers [35].

3.3. Effect of co-feeding food waste on pyrolysis of disposable face mask

The co-feeding food waste to pyrolysis of the single-use face mask affected the overall mass balances of the pyrolytic products. As seen in Fig. 1, the pyrolysis of the single-use face mask did not remain any solid product (i.e., char). However, the addition of food waste to the feedstock resulted in char ranging from 6.6 wt% to 26.3 wt% for the co-pyrolysis of the single-use face mask and food waste (Fig. 4). As more food waste was added to the feedstock, more char was produced at all temperatures tested. This clearly indicates that the char originates from the food waste. The char yields tend to decrease with the temperature increases, because the cleavage of –OH groups and C–H bonds is enhanced at elevated temperatures [36,37]. The non-condensable gas yield increases with an increase in the pyrolysis temperature for all five feedstocks. For instance, the non-condensable gas yield obtained with the 75% food waste/25% mask increases from 9.5 wt% to 16.6 wt% as the temperature increases from 773 K to 1173 K. This could be because thermal cracking of pyrolytic vapor is enhanced via homogeneous reactions taking place in the gas phase and heterogeneous reactions taking place in the gas–solid phase with a rise in the temperature [28,29].

The yield of non-condensable gases increased with increasing food waste loading in the feedstock (Fig. 4). Fig. 5 shows the volumetric proportion of non-condensable gases evolved from the pyrolysis of the mixtures of single-use face mask and food waste with different feed ratios at a range of temperatures. For the pyrolysis of the disposable face mask with co-feeding food waste, CO_2 was most produced non-condensable permanent gas, unlike the case of the pyrolysis of the single-use face mask without food waste. At all temperatures tested, the contents of CO_2 and CO in the pyrolytic gas tend to be proportional to the food waste loading in

Table 1
Results of proximate, ultimate, and composition analysis of the single-use mask and food waste.

wt.%	Mask	Food waste
Proximate analysis		
Moisture	0	3.3
Volatile matter	81.3	71.3
Fixed matter	9.2	15.1
Ash	9.5	10.3
Ultimate analysis		
C	75.9	47.5
H	14.9	6.6
O (by difference)	8.4	41.6
N	0.8	3.9
S	N.D.	0.4
Composition		
Cellulose	–	2.0
Hemicellulose	–	1.2
Lignin	–	0.1
Extractives	–	96.7

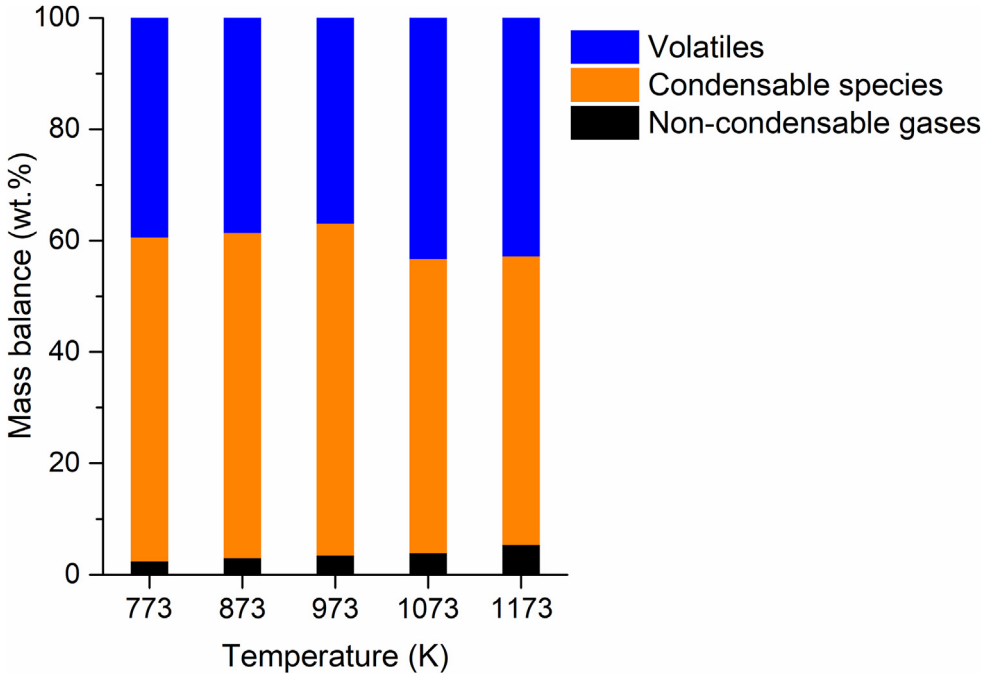

Fig. 1. Overall mass balances of the pyrolytic products produced via pyrolysis of the single-use face mask as a function of pyrolysis temperature.

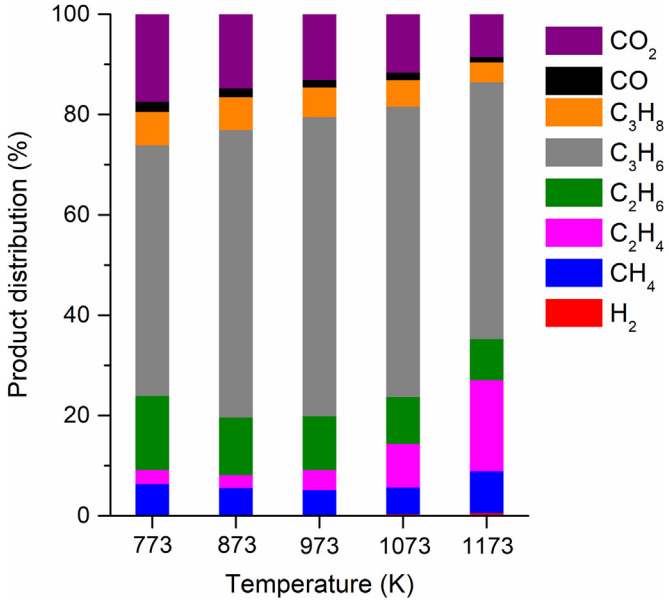

Fig. 2. Product distributions of non-condensable gases in the pyrolytic gas produced via pyrolysis of the single-use face mask as a function of pyrolysis temperature.

Table 2
Yields (wt.%; on the basis of weight of the feedstock) of the identified hydrocarbons with different carbon numbers, obtained from the pyrolysis of the single-use face mask at different pyrolysis temperatures.

Carbon number of hydrocarbons	Temperature (K)				
	773	873	973	1073	1173
C6	1.0	1.6	2.0	1.8	1.5
C10	1.1	1.2	1.7	1.1	1.0
C11	1.7	1.9	2.6	1.6	1.5
C12	5.8	6.2	8.3	5.9	5.3
C13	2.0	2.0	2.6	1.9	1.7
C14	0.8	1.0	1.1	1.2	1.3
C15	0.2	0.2	0.3	0.2	0.2
C16	6.9	7.2	8.3	7.7	7.8
C17	1.4	1.7	2.0	2.1	2.4
C18	1.0	1.3	1.5	1.3	1.3
C20	2.8	3.0	3.5	3.1	3.1
C22	0.4	0.5	0.6	0.5	0.5
C23	4.0	4.1	4.9	3.8	3.8
C25	3.6	3.8	4.2	4.0	4.0
C28	2.6	3.0	3.4	3.2	3.4

the feedstock, while the contents of C1–C3 hydrocarbons in the pyrolytic gas tend to be inversely proportional to the food waste loading in the feedstock. This is because of a high oxygen content of food waste, as seen in Table 1. The C1–C3 hydrocarbons are considered to originate primarily from polypropylene that constitutes the mask, so a higher food waste loading in the feedstock led to a lower content of C1–C3 hydrocarbons in the pyrolytic gas. Of the non-condensable gases, the change in H_2 proportion by varying both the pyrolysis temperature and the ratio of the single-use face mask to food waste is most considerable (Fig. 5). For all five feedstocks, the H_2 proportion increases with an increase in the pyrolysis temperature. At all tested temperatures, the H_2 proportion increases as the food waste loading in the feedstock increases from 0% to 75% (i.e., decrease in the single-use face mask loading from 100% to 25%). The H_2 proportion in the pyrolytic gas evolved from the pyrolysis of food waste only (i.e., food waste loading of 100%) is 20–80% lower than that in the pyrolytic gas evolved from the co-pyrolysis of 75% food waste and 25% single-use face mask (i.e., food waste loading of 75%).

Pyrolysis of solid biomass (e.g., food waste) particles occurs through three stages: drying, primary pyrolysis, and secondary pyrolysis [38]. In the drying stage, the biomass particles are heated locally, evaporating moisture, following primary pyrolysis. Thermal scission of chemical bonds in cellulose, hemicellulose, lignin, and extractives in the biomass takes place in the primary pyrolysis stage, releasing pyrolytic volatiles comprising non-condensable gases and some organic species that are condensable at ambient

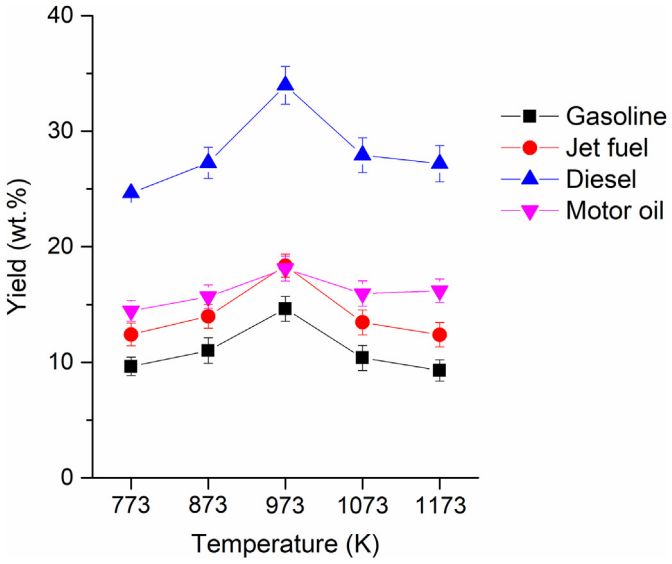

Fig. 3. Yields of different fuels and oils (on the basis of weight of the feedstock) produced via pyrolysis of the single-use face mask as a function of pyrolysis temperature.

conditions). Non-volatile pyrolytic solid (i.e., char) is yielded in the primary step. When the pyrolysis proceeds further, the volatiles evolved from the primary pyrolysis undergo parallel and serial reactions occurring homogeneously or heterogeneously (dehydration, dehydrogenation, condensation, polymerization, reforming, cracking, etc.), which result in the formation of a complex mixture of pyrolytic products. The char yielded in the primary step can be further transformed to H_2 in the secondary pyrolysis stage (i.e., dehydrogenation takes place). The secondary pyrolysis occurs at higher temperatures than the primary pyrolysis [39].

As mentioned above, the increase in pyrolysis temperature led to enhancing H_2 production for the co-pyrolysis of the single-use face mask and food waste. This is most likely because the reactions involved in the secondary pyrolysis (e.g., dehydrogenation of species evolved from food waste during its pyrolysis) readily occur at elevated temperatures [40,41]. Co-feeding the single-use face mask with food waste enhanced the H_2 production, compared to pyrolysis of the mask or food waste only at the temperatures tested. Two possible mechanisms of the co-feeding effect are available. First, the single-use face mask can serve as hydrogen donor during the co-pyrolysis [42,43], attributed to a higher H content of the mask than the food waste (Table 1). Second, water formed from the pyrolysis of food waste can act as a reactive compound that promotes thermal cracking of the pyrolytic vapor from the mask, thereby producing more volatile compounds such as H_2 [43,44].

The co-pyrolysis of the single-use face mask and food waste led to the formation of a variety of condensable species that can be classified as phenolic compounds, polycyclic aromatic hydrocarbons (PAHs) and their derivatives, hydrocarbons ranging from C6 to C28, N-containing species, and oxygenates involving acids, esters, alcohols, aldehydes, and ketones. Individual species that could be identified by the GC–MS analysis are listed in Table S6. Phenolic compounds are potentially carcinogenic, and they are toxic and

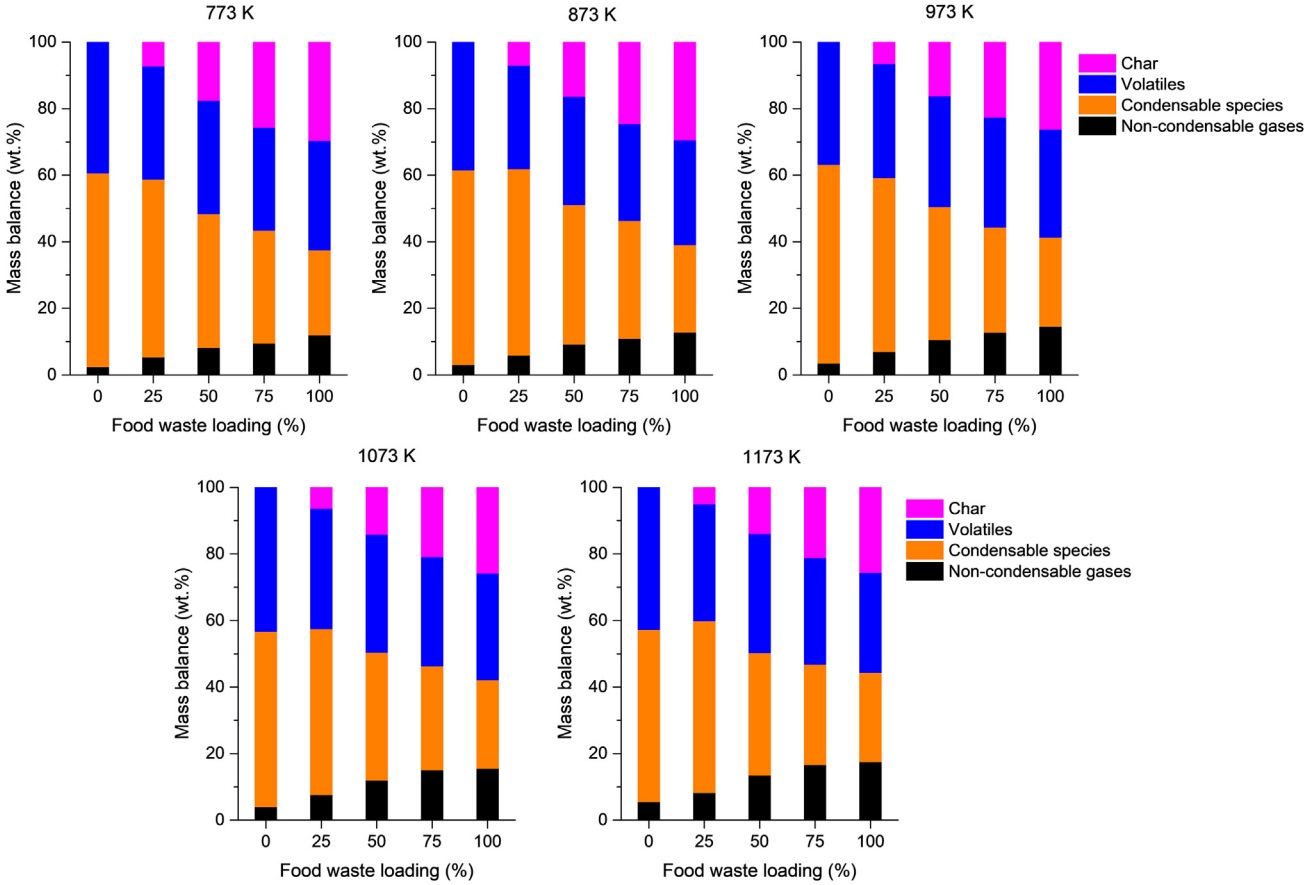

Fig. 4. Overall mass balances of the pyrolytic products produced via co-pyrolysis of the single-use face mask and food waste at a range of temperatures as a function of food waste loading in the feedstock.

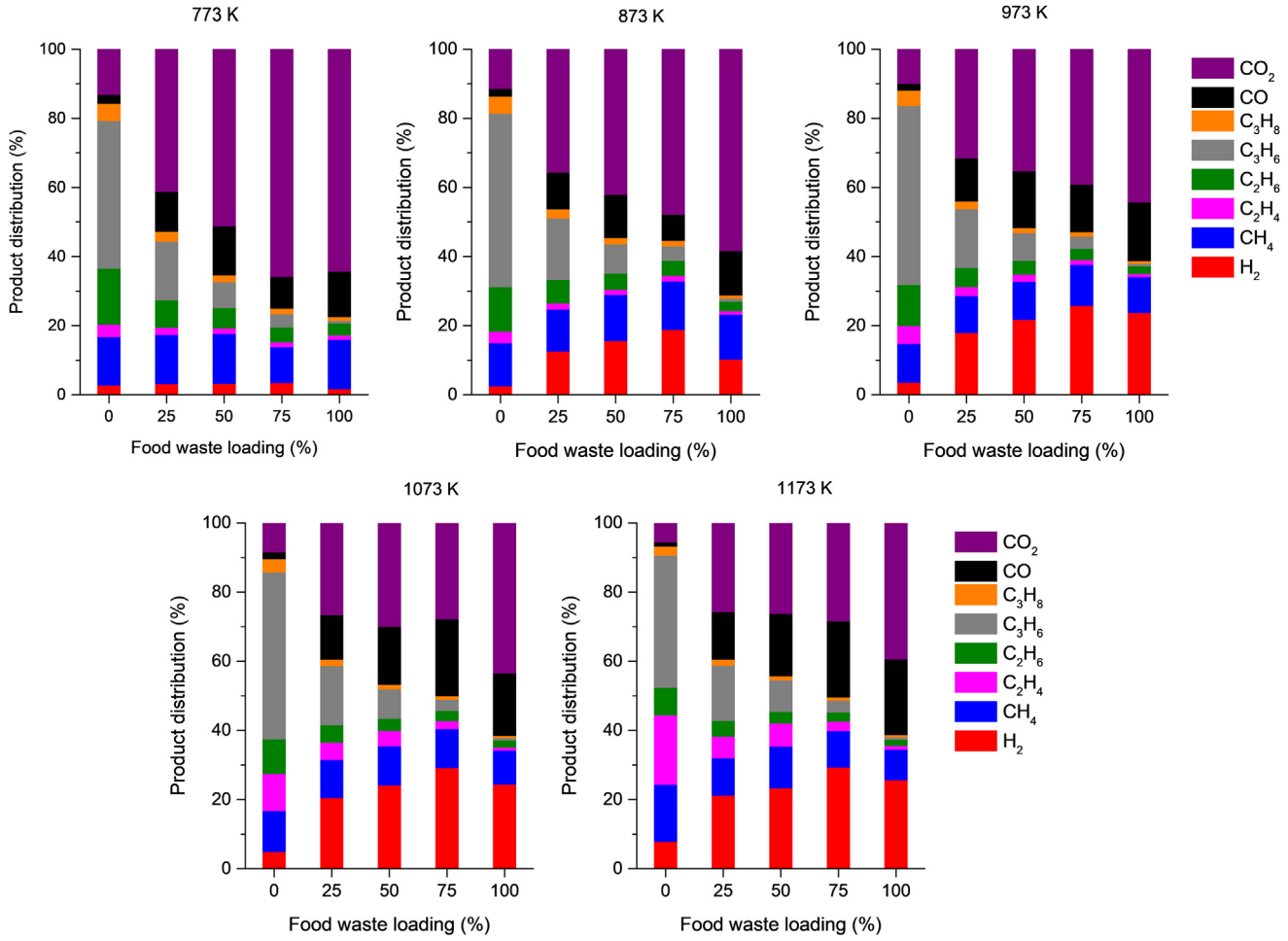

Fig. 5. Product distributions (volume basis) of non-condensable gases in the pyrolytic gas produced via co-pyrolysis of the single-use face mask and food waste at a range of temperatures as a function of food waste loading in the feedstock.

lethal to fish at low concentrations [45]. United States Environmental Protection Agency (US EPA) has designated phenol and phenolic compounds as priority pollutants taking 11th place among 126 undesirable chemicals [46,47]. PAHs and their derivatives are mutagenic and carcinogenic, cause heart disease, and damage to internal organs like kidney and liver [48]. Reactions between PAHs and ozone and nitrogen oxides lead to the formation of particulate oxygenated-PAHs that are considered a secondary organic aerosol [49]. PAHs and their derivatives can be generated from phenolic compounds and other benzene derivatives via the hydrogen atom abstraction, acetylene addition, and Diels-Alder mechanisms [50]. The acids involved in the oxygenates were mostly fatty acids originating from food waste. The esters may be generated via transesterification of the fatty acids. Alcohols, aldehydes, and ketones are commonly found in bio-oil produced via biomass pyrolysis [51].

Fig. 6 summarizes the results of condensable compounds according to the classification. The proportions of phenolic compounds and PAHs increases with an increase in the food waste loading in the feedstock. This is most likely because food waste contains lignin and extractives (Table 1) [52]. An increase in the pyrolysis temperature at a comparable food waste loading in the feedstock tended to increase the proportion of phenolic compounds and PAHs in the pyrolytic product. It is known that the formation of PAHs favors more at higher temperatures [53]. In addition, phenolic compounds could be better transformed to PAH derivatives at higher temperatures. The proportions of phenolic compounds and PAH derivatives increase with increasing the food waste loading in the feedstock. This was likely ascribed to the presence of lignin and extractives in the food waste (Table 1). The proportion of N-containing species increases either with increasing pyrolysis temperature or with increasing the food waste loading in the feedstock. This is ascribed to a higher N content of the food waste than that of the single-use face mask (Table 1). The proportion of oxygenates increases as the food waste loading in the feedstock increases because the fatty acids and esters mostly comprising the oxygenates originate from food waste, and the food waste has a four times higher O content than the single-use face mask. The addition of food waste to the feedstock dramatically decreases the proportion of hydrocarbons. As shown in Table 1, the food waste is composed of various substances. Thermal cracking of food waste leads to the formation of a mixture of a wide range of chemical species (mostly oxygenates) likely attributed to its complex heterogeneous nature and high oxygen content [54,55]. Therefore, the pyrolysis of the disposable face mask with co-feeding food waste decreased the yields of the hydrocarbons.

Char is non-volatile carbon-rich solid remained after pyrolysis, which can be exploited in a variety of applications such as fuel and structural materials. Thus, characterization of the chars produced via co-pyrolysis of the single-use face mask and food waste would be beneficial for the potential use of the materials. Table 3 lists specific surface area, total pore volume, average pore diameter,

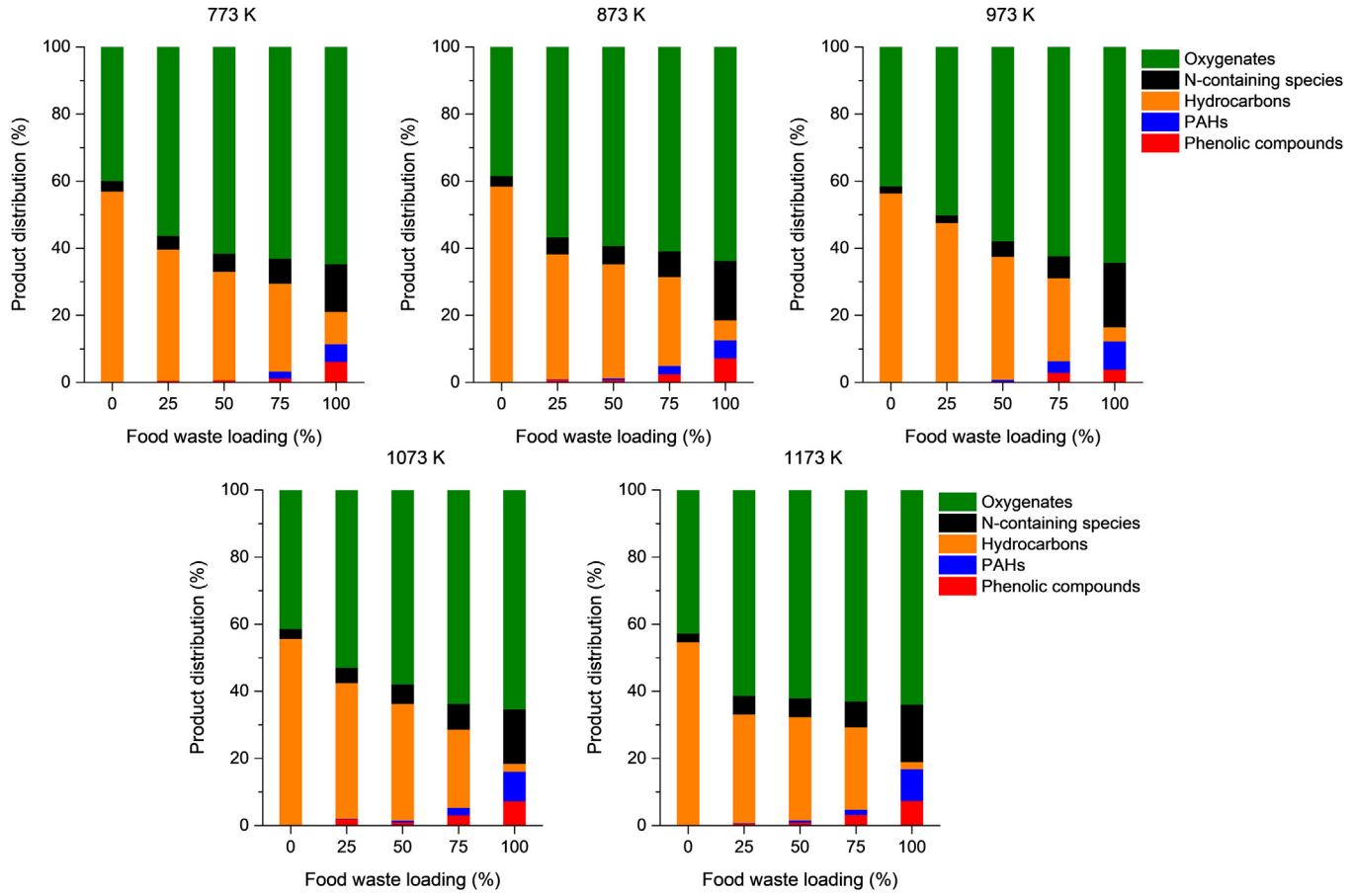

Fig. 6. Product distributions (mass basis) of condensable species in the pyrolytic liquid produced via co-pyrolysis of the single-use face mask and food waste at a range of temperatures as a function of food waste loading in the feedstock.

elemental composition, ash content, and HHV of the chars. The textual properties and HHV of the chars are not significantly different, likely because they originate from same food waste. This also means that the presence of the disposable face mask has negligible effect on the surface area, porosity, and energy content of the char.

4. Conclusions

In this study, the single-use face mask was pyrolyzed as a strategy to make fuel-range chemicals from everyday waste such as personal protective equipment against COVID-19. The effect of co-feeding food waste on the pyrolysis of the disposable face mask was investigated. The total yields of non-condensable permanent gases, composed primarily of CH_4, C_2H_6, C_3H_8, C_2H_4, and C_3H_6, obtained with the disposable face mask increased with an increase in pyrolysis temperature from 773 K to 1173 K. The HHV of the pyrolytic gas >40 MJ kg^{-1}. No char was formed for the pyrolysis of the single-use face mask. In addition to the non-condensable gases, hydrocarbons with different carbon number ranges (e.g., gasoline-, jet fuel-, diesel-, and motor oil-range hydrocarbons) were produced in the pyrolysis of the single-use face mask. The pyrolysis of the disposable face mask performed at 973 K led to the highest yields of gasoline-, jet fuel-, diesel-, and motor oil-range hydrocarbons (14.7 wt%, 18.4 wt%, 34 wt%, and 18.1 wt%, respectively). Co-feeding food waste affected the pyrolytic products of the disposable face mask. The co-pyrolysis of the single-use mask and food waste formed char resulting from the food waste. The presence of the single-use face mask negligibly affected specific surface area, porosity, and HHV of the char. The pyrolysis of the disposable face mask with co-feeding food waste produced more H_2 and less hydrocarbons, ascribed to the complex heterogeneous nature and

Table 3
Textural properties, elemental composition and ash content, and HHV of the chars made via co-pyrolysis of the single-use face mask and food waste at 973 K as a function of food waste loading in the feedstock.

Food waste loading (%)	Textual properties			Elemental composition and ash content (wt.%)					HHV (MJ kg^{-1})
	Surface area (m^2 g^{-1})	Total pore volume (cm^3 g^{-1})	Average pore diameter (nm)	C	H	O	N	Ash	
25	16.4	0.042	9.0	45.3	2.4	39.0	4.1	9.2	14.4
50	15.7	0.045	8.4	49.6	2.5	31.0	4.3	12.6	16.7
75	14.9	0.043	8.7	55.3	3.7	20.5	4.7	15.8	21.1
100	15.9	0.038	8.4	53.5	2.7	28.4	4.5	10.9	18.6

high oxygen content of the food waste. The addition of food waste to the pyrolysis of single-use face mask brings the benefit of a higher yield of pyrolytic gas with enhanced H_2 production. The data reported in this paper should be valuable for practical purpose. To understand more thoroughly the effects of co-feeding food waste on the production of fuel-range chemicals via pyrolysis of disposable face mask, the co-pyrolysis of single-use face mask and food waste needs to be mechanistically modeled.

Author statement

Chanyeong Park: Conceptualization, Investigation, Writing – original draft; **Heeyoung Choi**: Investigation; **Kun-Yi Andrew Lin**: Validation, Visulaization; **Eilhann E. Kwon**: Investigation, Methodology, Writing – review & editing; **Jechan Lee**: Supervision, Writing – original draft, Writing – review & editing.

Declaration of competing interest

The authors declare that they have no known competing financial interests or personal relationships that could have appeared to influence the work reported in this paper.

Acknowledgements

This work was supported by a National Research Foundation of Korea (NRF) grant, funded by the Korean Government (Ministry of Science and ICT) (No. NRF-2020R1C1C1003225).

Appendix A. Supplementary data

Supplementary data to this article can be found online at https://doi.org/10.1016/j.energy.2021.120876.

References

[1] Grand View Research. Disposable face mask market size, share & trends analysis report by product (protective, dust, non-woven), by application (industrial, personal), by distribution channel, and segment forecasts. 2020. 2027. 2020.
[2] United Nations. Five things you should know about disposable masks and plastic pollution. 2020.
[3] Prata JC, Silva ALP, Walker TR, Duarte AC, Rocha-Santos T. COVID-19 pandemic repercussions on the use and management of plastics. Environ Sci Technol 2020;54(13):7760–5.
[4] Bondaroff TP, Cooke S. Masks on the Beach: the impact of COVID-19 on marine plastic pollution. In: Stokes G, editor. OceansAsia; 2020.
[5] FAO. Food wastage footprint: impacts on natural resources. Rome: Food and Agriculture Organization of the United Nations (FAO); 2013.
[6] Bajželj B, Richards KS, Allwood JM, Smith P, Dennis JS, Curmi E, Gilligan CA. Importance of food-demand management for climate mitigation. Nat Clim Change 2014;4(10):924–9.
[7] Roe S, Streck C, Weiner P-H, Obersteiner M, Frank S. How improved land use can contribute to the 1.5°C goal of the Paris agreement. In: Working paper prepared by climate Focus and the international Institute for applied systems analysis; 2017.
[8] Lee Y, Kim S, Lee J. Co-pyrolysis for the valorization of food waste and oriental herbal medicine byproduct. J Anal Appl Pyrolysis 2021;154:105016.
[9] Ryu S, Lee J, Reddy Kannapu HP, Jang S-H, Kim Y, Jang H, Ha J-M, Jung S-C, Park Y-K. Acid-treated waste red mud as an efficient catalyst for catalytic fast copyrolysis of lignin and polyproylene and ozone-catalytic conversion of toluene. Environ Res 2020;191:110149.
[10] Kim S, Kwon EE, Kim YT, Jung S, Kim HJ, Huber GW, Lee J. Recent advances in hydrodeoxygenation of biomass-derived oxygenates over heterogeneous catalysts. Green Chem 2019;21(14):3715–43.
[11] Park Y-K, Ha J-M, Oh S, Lee J. Bio-oil upgrading through hydrogen transfer reactions in supercritical solvents. Chem Eng J 2021;404:126527.
[12] Kwon EE, Lee T, Ok YS, Tsang DCW, Park C, Lee J. Effects of calcium carbonate on pyrolysis of sewage sludge. Energy 2018;153:726–31.
[13] Jung J-M, Oh J-I, Baek K, Lee J, Kwon EE. Biodiesel production from waste cooking oil using biochar derived from chicken manure as a porous media and catalyst. Energy Convers Manag 2018;165:628–33.
[14] Uzoejinwa BB, He X, Wang S, El-Fatah Abomohra A, Hu Y, Wang Q. Co-pyrolysis of biomass and waste plastics as a thermochemical conversion technology for high-grade biofuel production: recent progress and future directions elsewhere worldwide. Energy Convers Manag 2018;163:468–92.
[15] Abnisa F, Wan Daud WMA. A review on co-pyrolysis of biomass: an optional technique to obtain a high-grade pyrolysis oil. Energy Convers Manag 2014;87:71–85.
[16] Kumar Mishra R, Mohanty K. Co-pyrolysis of waste biomass and waste plastics (polystyrene and waste nitrile gloves) into renewable fuel and value-added chemicals. Carbon Resour Convers 2020;3:145–55.
[17] Jung S, Lee S, Dou X, Kwon EE. Valorization of disposable COVID-19 mask through the thermo-chemical process. Chem Eng J 2021;405:126658.
[18] Lee SB, Lee J, Tsang YF, Kim Y-M, Jae J, Jung S-C, Park Y-K. Production of value-added aromatics from wasted COVID-19 mask via catalytic pyrolysis. Environ Pollut 2021;283:117060.
[19] Lin H-T, Huang M-S, Luo J-W, Lin L-H, Lee C-M, Ou K-L. Hydrocarbon fuels produced by catalytic pyrolysis of hospital plastic wastes in a fluidizing cracking process. Fuel Process Technol 2010;91(11):1355–63.
[20] Paraschiv M, Kuncser R, Tazerout M, Prisecaru T. New energy value chain through pyrolysis of hospital plastic waste. Appl Therm Eng 2015;87:424–33.
[21] Honus S, Kumagai S, Fedorko G, Molnár V, Yoshioka T. Pyrolysis gases produced from individual and mixed PE, PP, PS, PVC, and PET—part I: production and physical properties. Fuel 2018;221:346–60.
[22] Praveen Kumar K, Srinivas S. Catalytic co-pyrolysis of biomass and plastics (polypropylene and polystyrene) using spent FCC catalyst. Energy Fuels 2020;34(1):460–73.
[23] Jenkins N, Ekanayake J. 8. Bioenergy. Renewable energy engineering. United Kingdom: Cambridge University Press; 2017.
[24] Pleissner D, Lam WC, Sun Z, Lin CSK. Food waste as nutrient source in heterotrophic microalgae cultivation. Bioresour Technol 2013;137:139–46.
[25] Pleissner D, Kwan TH, Lin CSK. Fungal hydrolysis in submerged fermentation for food waste treatment and fermentation feedstock preparation. Bioresour Technol 2014;158:48–54.
[26] Karmee SK, Lin CSK. Valorisation of food waste to biofuel: current trends and technological challenges. Sustain Chem Process 2014;2(1):22.
[27] Mansor AM, Lim JS, Ani FN, Hashim H, Ho WS. Characteristics of cellulose, hemicellulose and lignin of MD2 pineapple biomass. Chem Eng Trans 2019;72:79–84.
[28] Nasir Uddin M, Daud WMAW, Abbas HF. Potential hydrogen and non-condensable gases production from biomass pyrolysis: insights into the process variables. Renew Sustain Energy Rev 2013;27:204–24.
[29] Hossain MA, Jewaratnam J, Ganesan P, Sahu JN, Ramesh S, Poh SC. Microwave pyrolysis of oil palm fiber (OPF) for hydrogen production: parametric investigation. Energy Convers Manag 2016;115:232–43.
[30] Dixon RE. United States patent 3485890A. 1969.
[31] Jun J-W, Kim T-W, Il Hong S, Kim J-W, Jhung SH, Kim C-U. Selective and stable production of ethylene from propylene over surface-modified ZSM-5 zeolites. Catal Today 2018;303:86–92.
[32] Choudhary VR, Rane VH, Rajput AM. Simultaneous thermal cracking and oxidation of propane to propylene and ethylene. AIChE J 1998;44(10):2293–301.
[33] Cho S-H, Lee SS, Jung S, Park Y-K, Lin K-YA, Lee J, Kwon EE. Carbon dioxide-cofeeding pyrolysis of pine sawdust over nickle-based catalyst for hydrogen production. Energy Convers Manag 2019;201:112140.
[34] Shen DK, Gu S. The mechanism for thermal decomposition of cellulose and its main products. Bioresour Technol 2009;100(24):6496–504.
[35] Audran G, Marque SRA, Siri D, Santelli M. Enthalpy of combustion on *n*-alkanes. quantum chemical calculations up to n-$C_{60}H_{122}$ and power law distributions. ChemistrySelect 2018;3(31):9113–20.
[36] Demirbas A. Effects of temperature and particle size on bio-char yield from pyrolysis of agricultural residues. J Anal Appl Pyrolysis 2004;72(2):243–8.
[37] Li S, Barreto V, Li R, Chen G, Hsieh YP. Nitrogen retention of biochar derived from different feedstocks at variable pyrolysis temperatures. J Anal Appl Pyrolysis 2018;133:136–46.
[38] Neves D, Thunman H, Matos A, Tarelho L, Gómez-Barea A. Characterization and prediction of biomass pyrolysis products. Prog Energy Combust Sci 2011;37(5):611–30.
[39] Shen Y, Ma D, Ge X. CO_2-looping in biomass pyrolysis or gasification. Sustain Energy Fuels 2017;1(8):1700–29.
[40] Kim S, Lee J. Pyrolysis of food waste over a Pt catalyst in CO_2 atmosphere. J Hazard Mater 2020;393:122449.
[41] Kim S, Lee Y, Andrew Lin K-Y, Hong E, Kwon EE, Lee J. The valorization of food waste via pyrolysis. J Clean Prod 2020;259:120816.
[42] Sonobe T, Worasuwannarak N, Pipatmanomai S. Synergies in co-pyrolysis of Thai lignite and corncob. Fuel Process Technol 2008;89(12):1371–8.
[43] Liu W-J, Tian K, Jiang H, Zhang X-S, Yang G-X. Preparation of liquid chemical feedstocks by co-pyrolysis of electronic waste and biomass without formation of polybrominated dibenzo-p-dioxins. Bioresour Technol 2013;128:1–7.
[44] Li C-Z, Nelson PF. Fate of aromatic ring systems during thermal cracking of tars in a fluidized-bed reactor. Energy Fuels 1996;10(5):1083–90.
[45] Abha S, Singh CS. Hydrocarbon pollution: effects on living organisms, remediation of contaminated environments, and effects of heavy metals co-contamination on bioremediation. In: Romero-Zerón L, editor. Introduction to enhanced oil recovery (EOR) processes and bioremediation of oil-contaminated sites. IntechOpen; 2012.
[46] Raza W, Lee J, Raza N, Luo Y, Kim K-H, Yang J. Removal of phenolic compounds from industrial waste water based on membrane-based technologies. J Ind

Eng Chem 2019;71:1–18.
[47] Yahaya A, Okoh OO, Agunbiade FO, Okoh AI. Occurrence of phenolic derivatives in buffalo river of eastern cape South Africa: exposure risk evaluation. Ecotoxicol Environ Saf 2019;171:887–93.
[48] Kim K-H, Jahan SA, Kabir E, Brown RJ. A review of airborne polycyclic aromatic hydrocarbons (PAHs) and their human health effects. Environ Int 2013;60:71–80.
[49] Lee HH, Choi NR, Lim HB, Yi SM, Kim YP, Lee JY. Characteristics of oxygenated PAHs in PM_{10} at seoul, Korea. Atmos Pollut Res 2018;9(1):112–8.
[50] Kislov VV, Islamova NI, Kolker AM, Lin SH, Mebel AM. Hydrogen abstraction acetylene addition and Diels–Alder mechanisms of PAH formation: a detailed study using first principles calculations. J Chem Theor Comput 2005;1(5):908–24.
[51] Diebold JP. A review of the chemical and physical mechanisms of the storage stability of fast pyrolysis bio-oils. Golden, Colorado, USA: National Renewable Energy Laboratory; 2000. No. NREL/SR-570-27613.
[52] Park C, Lee N, Kim J, Lee J. Co-pyrolysis of food waste and wood bark to produce hydrogen with minimizing pollutant emissions. Environ Pollut 2021;270:116045.
[53] Sharma RK, Hajaligol MR. Effect of pyrolysis conditions on the formation of polycyclic aromatic hydrocarbons (PAHs) from polyphenolic compounds. J Anal Appl Pyrolysis 2003;66(1):123–44.
[54] Oh J-I, Lee J, Lee T, Ok YS, Lee S-R, Kwon EE. Strategic CO_2 utilization for shifting carbon distribution from pyrolytic oil to syngas in pyrolysis of food waste. J CO2 Util 2017;20:150–5.
[55] Lee Y, Kim S, Kwon EE, Lee J. Effect of carbon dioxide on thermal treatment of food waste as a sustainable disposal method. J CO2 Util 2020;36:76–81.